processes

MDPI

Article

Preparation and Application of Coal-Liquefaction-Residue-Based Carbon Material

Liang Xu [1], Yizhe Lu [1], Nuerbiya Yalikun [1,2,*], Congchao Shi [1], Haoyang Wang [1], Yueyuan Xu [1] and Jie Liu [1]

[1] State Key Laboratory of Chemistry and Utilization of Carbon Based Energy Resources, Xinjiang Key Laboratory of Coal Cleaning Conversion & Chemical Engineering, Xinjiang Uyghur Autonomous Region, School of Chemical Engineering and Technology, Xinjiang University, Urumqi 830017, China
[2] College of Chemical Engineering, Xinjiang University, Urumqi 830017, China
* Correspondence: nuerbiya@xju.edu.cn; Fax: +86-9918-582-966

Abstract: P-Nitrophenol (4-NP) is a high toxicity material and has harmful effects on the environment. Thus, the analysis of 4-NP is an important topic at present. In this work, the fabrication of a novel electrochemical sensor based on coal-liquefaction-residue (CLR)-derived porous carbon (PC) materials. CLR-based porous carbon material was prepared by the high-temperature carbonization method and the morphology and structure of the materials were characterized by scanning electron microscopy and other characterization methods. Subsequently, the electrochemical properties of the modified electrodes were studied by cyclic voltammetry (CV) and differential pulse voltammetry (DPV) measurements. The results showed that under optimal conditions, the sensor had a good electrochemical performance for environmental pollutant 4-NP. In particular, the linear range of the sensor was 10–200 μmol·L-1 and the detection limit was 1.169 μmol·L^{-1} on the basis of the signal-to-noise ratio S/N = 3. The electrode showed excellent stability, reproducibility and repetitiveness and the sensor also had good selectivity. In addition, the newly constructed sensor exhibited adsorption-controlled kinetics and the recovery rate of 4-NP in actual water samples could reach 90.06~95.17%, indicating that the sensor had good practical application prospects.

Keywords: coal liquefaction residue; activation; carbon material; electrochemical sensor; p-nitrophenol

Citation: Xu, L.; Lu, Y.; Yalikun, N.; Shi, C.; Wang, H.; Xu, Y.; Liu, J. Preparation and Application of Coal-Liquefaction-Residue-Based Carbon Material. *Processes* **2022**, *10*, 2455. https://doi.org/10.3390/pr10112455

Academic Editors: Monika Wawrzkiewicz and Anna Wołowicz

Received: 13 August 2022
Accepted: 5 October 2022
Published: 19 November 2022

1. Introduction

P-nitrophenol (4-NP) as a raw chemical material is widely used in the production of pesticides, rubber, explosives, fuel, medicine and other chemical products [1–3]. 4-NP is stable and soluble in water, and it is a highly toxic, carcinogenic and refractory pollutant [2,4,5]. 4-NP can enter the body through the skin and mucosa, respiratory tract and digestive tract, and an accumulation of a low concentration of 4-NP can also cause chronic poisoning, and high concentrations of 4-NP can cause acute poisoning leading to coma and death. Therefore, it is crucial to efficiently and sensitively detect 4-NP [6]. At present, the reported methods for the detection of 4-NP or nitro compounds mainly include spectrophotometry [7], fluorescence spectroscopy, high performance liquid chromatography mass spectrometry [8], capillary electrophoresis and so on [9,10]. However, these methods have many disadvantages such as them being expensive, having a long analysis time and having tedious analysis steps [11,12], which are limited in the process of analysis. Among them, the electrochemical method, due to its advantages of convenient operation, simple testing procedures, low cost, short analysis time, low limit of detection, high sensitivity, good reproducibility and stability [12,13], is widely used in the analysis of nitro compounds [14].

The selection of electrode materials with high catalytic activity is very important in the preparation of electrochemical sensors [15,16], and the properties of the electrode materials directly affects the sensitivity and stability of the detection methods [17]. Carbon-based materials are widely used in analytical and industrial electrochemistry, electrocatalysis, energy storage and other fields, due to their strong stability and special electronic properties

and excellent electrochemical performance. In the preparation of carbon materials, carbon sources usually come from organic matter such as coal, petroleum and their processing products, and materials with superior performance can be also obtained with some chemical and physical treatment. Among them, coal liquefaction residue (CLR) is a waste product in the direct liquefaction process of coal [18]. CLR accounts for 20–30 wt.% of the mass of raw coal [19] and is rich in polycyclic aromatic hydrocarbons and polyaromatic hydrocarbons and is a mixture which mainly consist of carbon, ash and sulfur. Therefore, CLR can be used as the preferred carbon source for the preparation of carbon materials. CLR used as a carbon precursor to prepare carbon materials can improve the high-value utilization of CLR and realize resource recycling. In recent years, as modified electrode material, porous carbon materials have been widely used in the fabrication of electrochemical sensors. In this work, CLR was used as carbon source and the prepared porous carbon materials were applied to the construction of the electrochemical sensor used to detect environmental pollutants such as 4-NP. Thus, the effective utilization of CLR is of great significance for improving the economy of the direct coal liquefaction process and realizing the clean and efficient utilization of coal.

China has abundant coal resources; the seven coal chemical industry bases in Xinjiang have 40% of the country's coal resources and reserves [20]. In this study, the abundant coal chemical waste CLR from Xinjiang was used to prepare a porous carbon material with good conductivity and good catalytic activity for 4-NP, which was used to fabricate a new electrochemical sensor for the rapid detection of 4-NP. The results showed that the electrochemical sensor showed high electrocatalytic activity, good selectivity and stability in the detection of 4-NP and had a wide detection range.

2. Experimental

2.1. Instrument and Materials

The following equipment was obtained: a CHI-840b electrochemical workstation (Shanghai Chenhua Instrument Company, Shanghai, China), scanning electron microscope (SEM, Hitachi SU−8010, Japan), transmission electron microscope (TEM, JEOL JEM-2100PLUS, Japan), vacuum drying oven (Shanghai Jinghong Experimental Equipment Co., Ltd., Shanghai, China), magnetic stirrer (Jintan Medical Instrument Factory, Jintan, China), ultrasonic cleaning machine (Kunshan Ultrasonic Instrument Co., Ltd., Kunshan, China) and tube furnace (Hefei Kojing Material Technology Co., Ltd., Hefei, China). The following materials were used: KOH, SBA-15 molecular sieve, polishing powder (0.3 μm and 0.05 μm Al_2O_3 powder), dilute hydrochloric acid (1 mol·L^{-1}), deionized water, sodium dihydrogen phosphate, disodium hydrogen phosphate, potassium ferricyanide, potassium ferrocyanide and isopropanol. All of these reagents were analytical grade, and deionized water was used for all solution preparations, and PBS buffer solution (0.1 mol·L^{-1}) was prepared with NaH_2PO_4 and Na_2HPO_4.

2.2. Preparation of CLR-Based Carbon Materials

The activator and template were the important factors in the preparation of the porous carbon materials. In this experiment, in order to effectively control the material structure, potassium hydroxide was used as the activator, because the KOH activation method can produce micropores and mesopores with a small pore size in various structural carbon materials and improve the microporous and mesoporous ratio of the material [21,22]. Furthermore, the mesoporous molecular sieve SBA-15 was used as the template, and subsequently a carbon precursor was introduced into the pore, and carbon material with porous structure was obtained by the high temperature carbonization method. Specifically, CLR (2 g), potassium hydroxide (6 g) and SBA-15 were fully ground in a mortar. The mixture was carbonized at a high temperature in a porcelain boat. The specific operation was as follows: the porcelain boat was put into the tube furnace, and nitrogen was used as a guard gas at a rate of 300 mL·min^{-1}; the tube furnace was heated to 800° at 5 °C·min^{-1} for direct carbonization for 3 h, and after cooling to room temperature, the porcelain boat was

removed. In order to remove the template, the sample was washed with an appropriate amount of 1 mol·L^{-1} dilute hydrochloric acid and dried in vacuum at 60 °C for 10 h. Finally, the obtained CLR-based carbon material was labeled as coal-liquefaction-residue-based porous carbon (CLR-PC) material. The schematic diagram of the preparation process is shown in Figure 1.

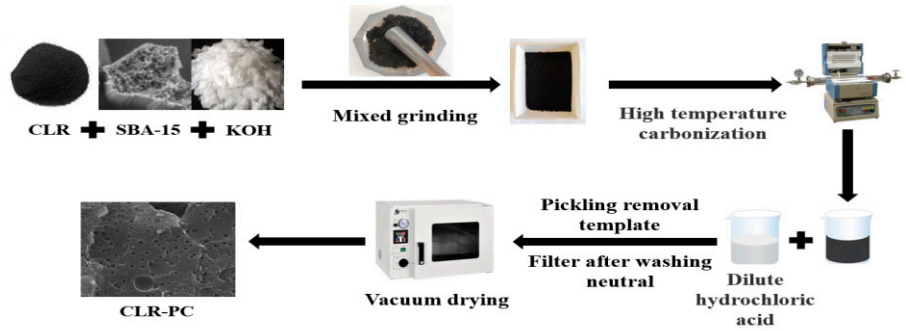

Figure 1. Schematic diagram of preparation of porous carbon based on coal liquefaction residue.

2.3. Preparation of ClR-PC/GCE

The preparation of the modified electrode was conducted as follows: the bare glassy carbon electrode (GCE, Φ = 3 mm) was polished on a pad with different specifications of aluminum oxide powder (1.0, 0.3, 0.05 μm), and then ultrasonically cleaned with absolute ethanol and deionized water successively. The CLR-PC was added to an isopropanol–aqueous solution and dispersed by ultrasonication. A homogeneous dispersion of the CLR-PC (5 μL) was evenly spread on the surface of pretreated bare GCE and dried naturally to obtain the CLR-PC/GCE.

3. Result and Discussion

3.1. Characterization of CLR-PC

The surface morphology and structure of the CLR-based carbon materials were analyzed and studied by SEM and TEM characterization as shown in Figure 2. Figure 2a is the SEM image of the original CLR, showing that the CLR had a non-porous structure on the surface, and Figure 2b is the SEM image of the CLR-PC after activation and high temperature carbonization with the template and alkali, where the surface had a disordered pore structure of different sizes, which facilitates the transfer of electrons on the electrode surface. In addition, the material had a significant honeycomb-shaped porous structure, indicating that the activation of strong bases was effective in deriving more developed pore structures. The TEM images of the CLR-PC (Figure 2c,d) further confirmed the porous structure of the CLR-PC material, which was consistent with SEM image.

3.2. Raman Spectrum of CLR-PC

Figure 3 shows the Raman spectra of the prepared CLR-PC samples. It shows a D and G peak at 1347 cm^{-1} and 1591 cm^{-1} respectively. This represents the characteristic absorption peak of disordered carbon and an ordered graphite structure. The peak intensity ratio (I_D/I_G) of peak D and peak G represented the graphitization degree of the carbon material. The I_D/I_G of CLR-PC was calculated as 1.04, indicating that it had a certain graphitization degree. The sample used as the electrode material had good electrical conductivity and a highly rated performance [23].

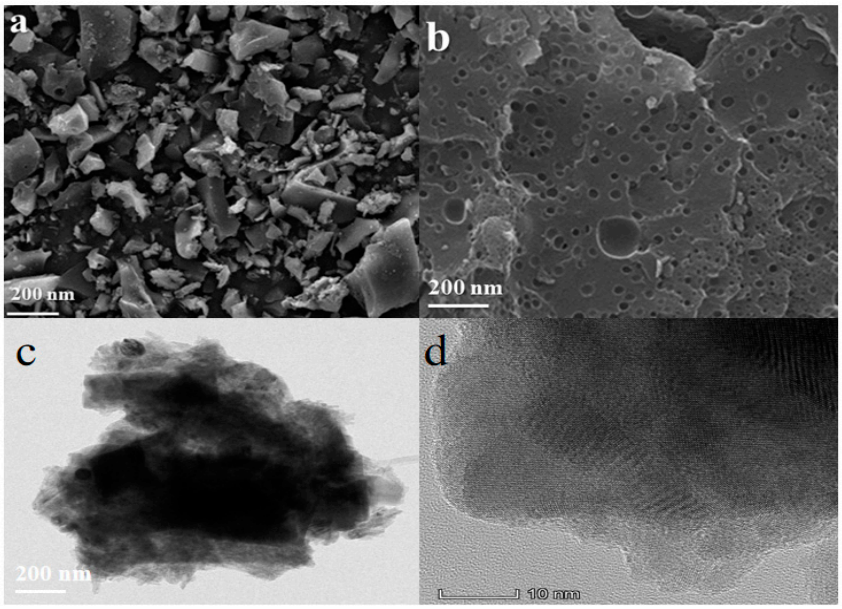

Figure 2. SEM images of (**a**) CLR and (**b**) CLR-PC materials, and TEM images of CLR-PC (**c**,**d**).

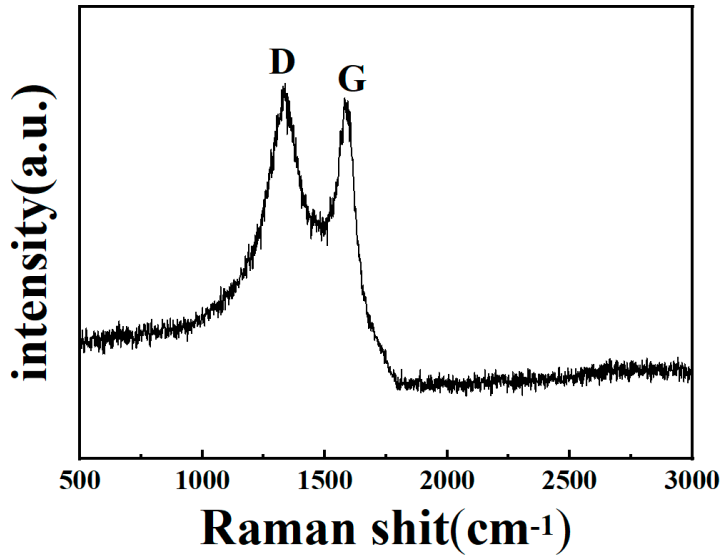

Figure 3. The Raman spectrum of CLR-PC.

3.3. Electrochemical Impedance of CLR-PC/GCE

Electrochemical impedance spectroscopy (EIS) was used to characterize the electrochemical impedance of the modified electrode. The separation efficiency of the carrier and the transfer of charge had a great influence on the 4-NP reduction. The results are shown in Figure 4. The smaller arc radius in the impedance diagram represents a more effective charge transfer effect, and it can be seen that the arc radius of the modified electrode was obviously smaller than that of the bare electrode, revealing that the CLR-PC had a better conductivity, which is beneficial for improving the charge separation efficiency and speeding up the reaction.

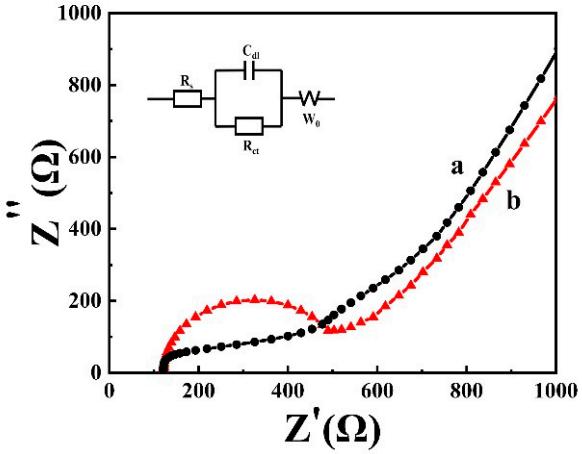

Figure 4. Electrochemical impedance spectra plots of CLR-PC/GCE (a) and GCE (b). Electrodes were in 1 mmol·L^{-1} $[Fe(CN)_6]^{3-/4-}$ containing 0.1 mol·L^{-1} KCl.

3.4. Electrochemical Behavior of 4-NP on CLR-PC/GCE

In order to study the electrochemical activity of the CLR-PC, the catalytic activity of 4-NP was tested with the CLR-PC/GCE-modified electrodes. Figure 5 shows the cyclic voltammetry (CV) of the bare GCE and CLR-PC/GCE. The test was performed in 0.1 mol·L^{-1} PBS (pH = 6) containing 4-NP. The characteristic peak of 4-NP appeared at −0.8 V for both electrodes (Figure 5), meaning that the nitro group went through a reduction reaction to form hydroxylamine [24]. The chemical reaction mechanism was given by Figure 5:

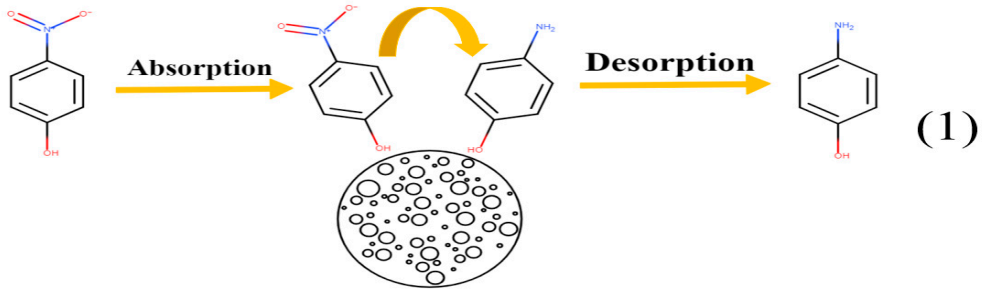

Figure 5. The electrode reaction mechanism of 4-NP on the CLR-PC/GCE.

The electrochemical peak current of 4-NP on the bare GCE surface was weak, and the characteristic peak current of the 4-NP on CLR-PC/GCE was apparently increased (Figure 6 line b), contributing to the fact that the CLR-PC materials had the advantage of excellent conductive and catalytic activity, in addition to the special porous structure of the CLR-derived carbon materials. This is beneficial to the adsorption of 4-NP on the surface of CLR-PC modified electrode. Therefore, the prepared electrochemical sensor had good electrocatalytic performance with regards to 4-NP, which should be further analyzed for its 4-NP correlation.

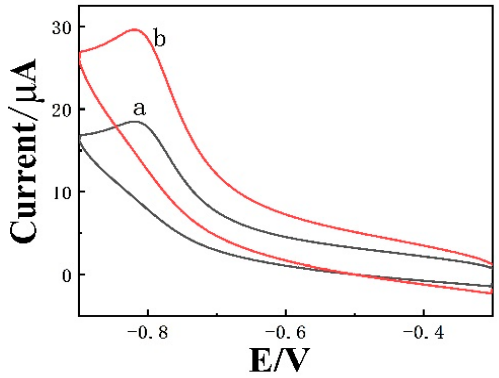

Figure 6. Cyclic voltammograms of 100μmol·L^{-1} 4-NP of bare GCE (a) and CLR-PC/GCE (b) in 0.1 mol·L^{-1} phosphate buffer (pH = 6).

3.5. Effects of Scan Rate

In order to investigate the reaction mechanism of 4-NP on the CLR-PC-modified electrode, the effect of the scan rate was investigated. Figure 6a shows the CV test results of the CLR-PC/GCE with 0.1 mol·L^{-1} PBS (pH = 6) containing a 100 μL 4-NP solution at different scan rates, ranging from 30~200 mV·s^{-1}. The results showed that the reduction peak current of the 4-NP increased with the increase in the scan rate, and Figure 7b shows the linear relationship, which was between the peak current and scan rate, as shown by the linear realtion was expressed as I_{pc}(μA) = 0.09698v(mV·s^{-1})−11.015 (R^2 = 0.9929), indicating that the 4-NP was controlled by adsorption on the surface of CLR-PC/GCE [25].

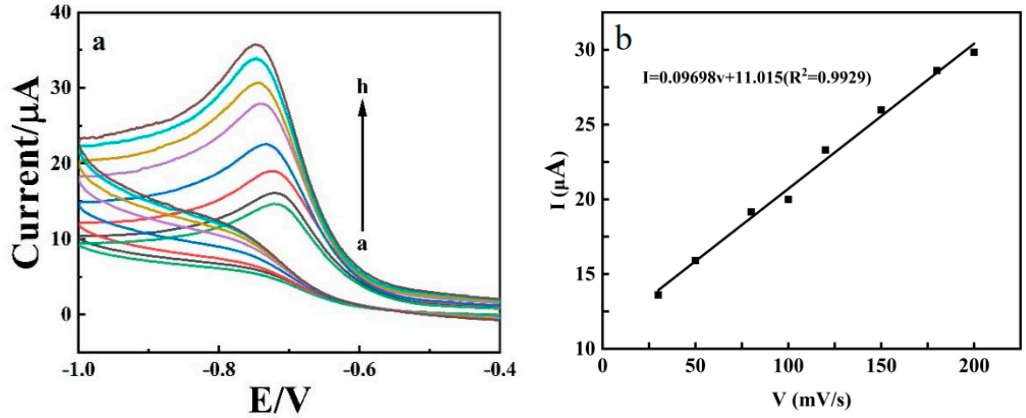

Figure 7. (**a**) CV curves of CLR-PC/GCE toward 100μmol·L^{-1}4-NP at different scan rates: 30, 50, 80, 100, 120, 150, 180 and 200 mV·s^{-1} (from a to h); (**b**) The calibration plot of peak current versus scan rate.

3.6. pH Effect

The effect of pH on the electrochemical detection capabilities of the electrochemical sensor towards 4-NP in 0.1 M PBS was investigated across the pH range of 5.0~9.0. (4.0, 5.0, 6.0, 7.0 and 8.0). It can be seen from Figure 8a that when the pH increased from 4.0 to 8.0, the peak current increased and then decreased, and the maximum value occurred at pH = 6. Therefore, a 0.1 mol·L^{-1} PBS buffer solution with pH = 6 was selected as the electrolyte solution. Figure 8c shows that, with the increase in pH, the reduction peak potential E_{pc} gradually shifted to the negative direction, and there was a linear relationship between the pH and peak potential. The regression equation is expressed as E_{pc} (V) = −0.3552–0.0558 pH (R^2 = 0.997), and the slope of the line −55.8 mV pH^{-1} was close to the Nernst equation at room temperature −59 mV pH^{-1}, indicating that the electrode reaction process of 4-NP on the modified electrode involved an equal number of protons and electrons [26].

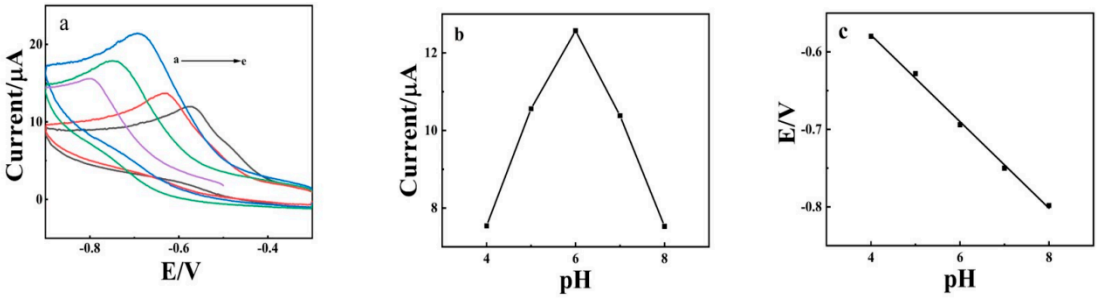

Figure 8. (**a**) Cyclic voltammograms of CLR-PC/GCE in 100 μmol·L^{-1} 4-NP at pH of 4.0, 5.0, 6.0, 7.0 and 8.0. Scan rate: 100 mv·s^{-1}. (**b**) Plot for the relationship between pH and peak current, and (**c**) plot for the relationship between pH and E_{pc}.

3.7. Electrochemical Determination of 4-NP

Under the optimal conditions, differential pulse voltammetry (DPV) was further carried out for the determination of 4-NP. As shown in Figure 9a, when the concentration of 4-NP varied from 10~200 μmol·L^{-1}, the peak current also increased with the increase in the concentration. Figure 8b shows the relationship between the peak current and concentration; when the 4-NP concentration varied from 10–200 μmol·L^{-1}, there was a linear relationship between the peak current and concentration, the linear regression equation was I(μA) = 0.3678C(μmol·L^{-1}) + 0.9946 (R^2 = 0.9956) and the detection limit was calculated as 1.169 μmol·L^{-1} ($C = 3\sigma/s$, σ is the standard deviation of the intercept of the concentration–current curve and s is the slope of the curve). In order to further verify the catalytic activity of the CLR-PC, the results were compared with previous research, and the comparison of the different electrochemical sensors for the detection of 4-NP is summarized in Table 1, which shows that the CLR-PC/GCE sensor had a large linear range and a low detection limit, and had certain detection advantages.

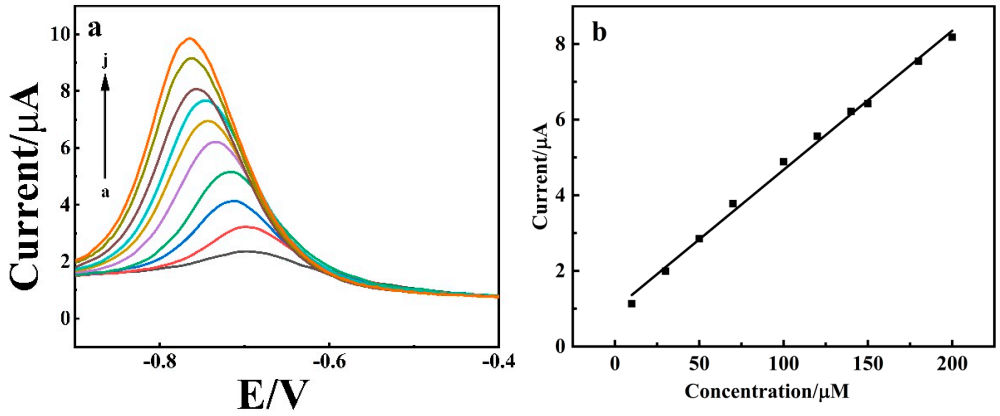

Figure 9. (**a**) DPV responses of CLR-PC/GCE in 0.1 mol·L^{-1} PBS (pH = 6.0) containing different concentrations of 4-NP (10–200 μmol·L^{-1}). Scan rate: 100 mV·s^{-1}. (**b**) The calibration plot of peak current versus concentration.

Table 1. Comparison of 4-NP determination between the present work and the reported methods.

Electrode Material	Linear Range (μmol·L^{-1})	Limit of Detection (μmol·L^{-1})	Reference
MWNT-Nafion/GCE [1]	10–620	1.3	[27]
AcSCD-AuNPs-MC [2]	0.1–350	26.1	[28]
p -NP-MIP-PANI/GO [3]	60–140	20	[29]
CLR-PC/GCE	10~200	1.169	This work

[1] Multiwalled carbon nanotube with naphthol-modified glassy carbon electrode. [2] Glassy carbon electrode modified with mesoporous carbon-gold nanoparticles and cyclodextrin. [3] Go—nano-structure-imprinted polyaniline-modified glassy carbon electrode.

3.8. Inferences Study

In order to investigate the selectivity of the CLR-PC/GCE, several common metal ions, inorganic anions and p-NP-like organic compounds were investigated in a certain concentration in this experiment. A total of 1000 μmol·L^{-1} of Na^+, Ni^+, K^+, Fe^{2+}, Fe^{3+}, Ca^{2+}, Zn^{2+}, Cl^{-1}, $PO_4{}^{2-}$, $NO_3{}^-$, $SO_4{}^{2-}$, o-nitrophenol, resorcinol and phenol were detected simultaneously with 4-NP (10μmol·L^{-1}). As seen from Figure 10, different interfering substances had a tiny influence on the peak current of 4-NP in the DPV detection, and the relative standard deviation (RSD) of the DPV response signal was calculated as 2.939%, indicating that the sensor had more resistant to interference.

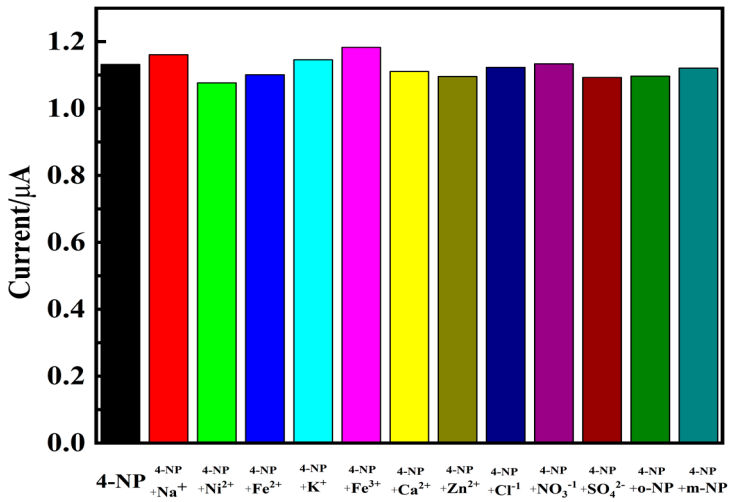

Figure 10. DPV response of 4-NP in 0.1 mol·L^{-1} PBS (pH = 6.0) at CLR-PC/GCE for different interference compounds.

3.9. Repeatability, Reproducibility and Stability of CLR-PC/GCE

Figure 11 shows the results of the repeatability, reproducibility and stability of the modified electrodes. Firstly, the solution containing 4-NP was tested 10 times in parallel using the same CLR-PC electrode, and the RSD of the multiple tests was 2.388%, indicating that the CLR-PC/GCE had good repeatability. In addition, ten modified electrodes were used to measure 4-NP, and the RSD was 3.275%, which revealed that the sensor had good reproducibility. Finally, the CLR-PC/GCE was stored at room temperature for two weeks, and the electrochemical signal of 4-NP on the electrode surface remained at 95% of the original value, and the relative RSD of the test results was 1.554%. Hence, the fabricated sensor had good stability for the accurate analysis of 4-NP.

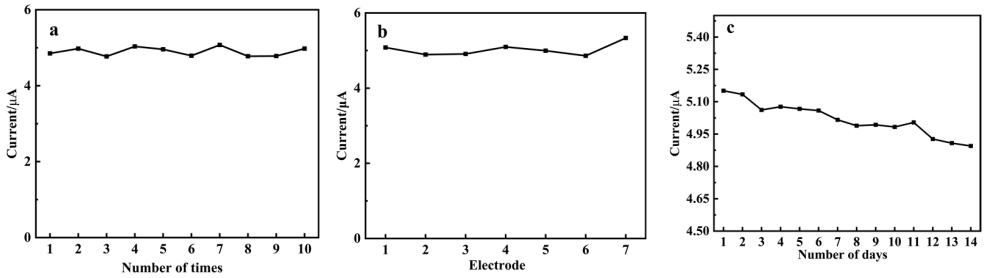

Figure 11. The reproducibility (**a**), repeatability (**b**) and stability (**c**) of CLR-PC/GCE.

3.10. Analytical Application

In order to research the potential applications of the constructed sensor, analytical performance was carried out by DPV measurements. The CLR-PC-modified GCE was used to measure the content of *4*-NP in tap water samples using standard addition methods for evaluating the feasibility of the fabricated sensor for real sample analysis. When 4-NP was

not added, there was no DPV signal. When different concentrations of 4-NP were added to the water sample, the corresponding peak current signal appeared. As shown in Table 2, recoveries ranging from 90.06% to 95.17% and RSD ranging from 1.904% to 2.67% for 4-NP revealed that the constructed electrochemical sensor had good practical applications and had potential applications in industrial and environmental sample analysis [30].

Table 2. Determination results of 4-NP in water samples and recovery value.

Sample	Injection ($\mu mol \cdot L^{-1}$)	Detection ($\mu mol \cdot L^{-1}$)	RSD (%, n = 3)	Recovery Efficiency (%)
Tap water	10	9.006	2.67%	90.06%
	30	28.183	1.904%	94.94%
	70	66.622	2.17%	95.17%

4. Conclusions

In summary, CLR-PC-modified GCE was applied for the selective and sensitive detection of 4-NP. Coal chemical waste CLR was used as a carbon precursor, and the CLR-based electrode materials were prepared by the template method with high-temperature carbonization and alkali activation. The CLR-PC-fabricated sensor could selectively recognize 4-NP by the electrochemical method, and it showed an excellent catalytic effect on the reduction of 4-NP. There was an exact linear relationship between the peak current and the concentration of 4-NP in the range of 10–200 $\mu mol \cdot L^{-1}$. Under optimal conditions, the CLR-PC/GCE also had high stability, sensitivity and reproducibility. In addition, the sensor had a high recovery for the detection of 4-NP in real tap water samples, with the recovery rate ranging from 90.06% to 95.15%. In a word, the synthesis method of CLR-PC was simple, the raw material was both easy to obtain and low cost, and the sample had good practical application abilities, showing that the fabricated sensor could be expected to be applied in the rapid and sensitive detection of 4-NP in other environmental samples.

Author Contributions: L.X.: writing, experiment, thingking; Y.L.: experiment; N.Y.: instructing, writing, supporting; C.S.: writing; H.W.: experiment; Y.X.: writing; J.L.: thingking. All authors have read and agreed to the published version of the manuscript.

Funding: Xinjiang University College Student Innovation Training Program (XJU-SRT-21079) and Natural Science Foundation of Xinjiang University.

Institutional Review Board Statement: Not applicable.

Informed Consent Statement: Not applicable.

Data Availability Statement: Data openly available in a public repository.

Acknowledgments: The authors gratefully acknowledge the financial support by the Xinjiang University College Student Innovation Training Program (XJU-SRT-21079) and Natural Science Foundation of Xinjiang University.

Conflicts of Interest: The authors declare that they have no known competing financial interests or personal relationships that could have appeared to influence the work reported in this paper.

References

1. Wei, Y.; Kong, L.T.; Yang, R.; Wang, L.; Liu, J.H.; Huang, J.X. Single-walled carbon nanotube/pyrenecyclodextrin nanohybrids for ultrahighly sensitive and selective detection of p-nitrophenol. *Langmuir* **2011**, *27*, 10295–10301. [CrossRef] [PubMed]
2. Rahman, M.M.; Sheikh, T.A.; Asiri, A.M.; Alamry, K.A.; Hasnat, M.A. Fabrication of an ultra-sensitive para-nitrophenol sensor based on facile Zn-doped Er_2O_3 nanocomposites via an electrochemical approach. *Anal. Methods* **2020**, *12*, 3470–3483. [CrossRef] [PubMed]
3. Jadoon, T.; Mahmood, T.; Ayub, K. Silver-graphene quantum dots based electrochemical sensor for trinitrotoluene and p-nitrophenol. *Mol. Liq.* **2020**, *306*, 112878–112890. [CrossRef]
4. Zhang, Y.; Xie, Q.; Xia, Z.; Gui, G.F.; Deng, F. Graphdiyne oxides as new modifier for the simultaneous electrochemical detection of phenolic compounds. *Electroanal. Chem.* **2020**, *863*, 114058–114088. [CrossRef]

5. Yu, M.Y.; Liu, J.H.; Liu, C.; Pei, W.Y.; Ma, J.F. Resorcin[4]arene-based microporous metal–organic framework/reduced graphene oxide composite as an electrocatalyst for effective and simultaneous determination of p-nitrophenol and o-nitrophenol isomers. *Sens. Actuators B Chem.* **2021**, *347*, 130604–130625. [CrossRef]
6. Mohanta, D.; Mahanta, A.; Mishra, S.R.; Jasimuddin, S.; Ahmaruzzaman, M. Novel SnO2@ZIF-8/gC3N4 nanohybrids for excellent electrochemical performance towards sensing of p-nitrophenol. *Environ. Res.* **2021**, *197*, 111077–111090. [CrossRef]
7. Li, Y.; Ma, Y.; Lichtfouse, E.; Song, J.; Gong, R.; Zhang, J.H.; Wang, S.; Xiao, L.L. In situ electrochemical synthesis of graphene-poly(arginine) composite for p-nitrophenol monitoring. *J. Hazard Mater.* **2022**, *421*, 126718–126727. [CrossRef]
8. Baikeli, Y.; Mamat, X.; Chen, L.; Liu, X.S.; Shen, L.; Luy, Y.; Li, C.H. Ultrasensitive and simultaneous determination of p-Nitrophenol and p-Nitrobenzoic acid by a modified glassy carbon electrode with N-rich nanoporous carbon derived from ZIF-8. *Electroanal. Chem.* **2021**, *899*, 115567–115585. [CrossRef]
9. Wang, Q.Z.; Li, R.; Zhao, Y.J.; Zhe, T.T.; Bu, T.; Liu, Y.N.; Sun, X.Y.; Hu, H.F.; Zhang, M.; Zheng, X.H.; et al. Surface morphology-controllable magnetic covalent organic frameworks: A novel electrocatalyst for simultaneously high-performance detection of p-nitrophenol and o-nitrophenol. *Talanta* **2020**, *219*, 121255–121286. [CrossRef]
10. Wei, W.; Yang, S.; Hu, H.H.; Li, H.; Jiang, Z.F. Hierarchically grown $ZnFe_2O_4$-decorated polyaniline-coupled-graphene nanosheets as a novel electrocatalyst for selective detecting p-nitrophenol. *Microchem. J.* **2021**, *160*, 105777–106791. [CrossRef]
11. Kaur, R.; Kaur, J.; Kumar, V.; Tikoo, K.B.; Rana, S.; Kaushik, A.; Singhal, S. Unfolding the electrocatalytic efficacy of highly conducting $NiFe_2O_4$-rGO nanocomposites on the road to rapid and sensitive detection of hazardous p-Nitrophenol. *Electroanal. Chem.* **2021**, *887*, 115161–115167.
12. Ata, S.; Feroz, M.; Bibi, I. Investigation of electrochemical reduction and monitoring of p-nitrophenol on imprinted polymer modified electrode. *Synth. Met.* **2022**, *287*, 117083–117099. [CrossRef]
13. Dib, M.; Moutcine, A.; Ouchetto, H. Novel synthesis of α-Fe_2O_3@Mg/Al-CO_3-LDH nanocomposite for rapid electrochemical detection of p-nitrophenol. *Inorg. Chem. Commun.* **2021**, *131*, 108788–108800. [CrossRef]
14. Cheng, X.L.; Xia, X.; Xu, Q.Q.; Wang, J.; Sun, J.C.; Zhang, Y.X.; Li, S.S. Superior conductivity FeSe2 for highly sensitive electrochemical detection of p-nitrophenol and o-nitrophenol based on synergistic effect of adsorption and catalysis. *Sens. Actuators B Chem.* **2021**, *348*, 130692–130704. [CrossRef]
15. Hofmann, D.; Hartmann, F.; Herrmann, H. Analysis of nitrophenols in cloud water with a miniaturized light-phase rotary perforator and HPLC-MS. *Anal. Bioanal. Chem.* **2008**, *391*, 161–169. [CrossRef] [PubMed]
16. Wang, X.; Li, M.; Yang, S. Self-assembled Ti3C2TX MXene/graphene composite for the electrochemical reduction and detection of p-nitrophenol. *Microchem. J.* **2022**, *179*, 107473–1007389. [CrossRef]
17. Karaová, J.; Barek, J.; Schwarzová-Pecková, K. Oxidative and Reductive Detection Modes for Determination of Nitrophenols by High-Performance Liquid Chromatography with Amperometric Detection at a Boron Doped Diamond Electrode. *Anal. Lett.* **2015**, *49*, 66–79. [CrossRef]
18. Li, X.; Zhao, Q.; Du, X. Synthesis of Carbon Nanofibers Film from Coal Liquefaction Residues: Effect of HNO3 Pretreatment. *Energy Fuels* **2022**, *36*, 4616–4624. [CrossRef]
19. Zhang, W.; Wilson, C.R.; Danielson, N.D. Indirect fluorescent determination of selected nitro-aromatic and pharmaceutical compounds via UV-photolysis of 2-phenylbenzimidazole-5-sulfonate. *Talanta* **2008**, *74*, 1400–1407. [CrossRef]
20. Zeng, Q.; Li, G.S.; Dong, J.X. Typical Ecological and Environmental Issues and Countermeasures in Coal Mining in Xinjiang Region. *Mining Saf. Environ. Prot.* **2017**, *44*, 106–110.
21. Yang, L.; Feng, Y.; Cao, M.; Yao, J. Two-step preparation of hierarchical porous carbon from KOH-activated wood sawdust for supercapacitor. *Mater. Chem. Phys.* **2019**, *238*, 121956. [CrossRef]
22. Guan, L.; Pan, L.; Peng, T.; Gao, C.; Wu, M. Synthesis of biomass-derived nitrogen-doped porous carbon nanosheests for high-performance supercapacitors. *ACS Sustain. Chem. Eng.* **2019**, *7*, 8405–8412. [CrossRef]
23. Tan, X.; Zhao, G.; Zhou, X.; Li, T.; Lei, H.; Du, G.; Yang, L. Electrochemical recognition of nitrophenol isomers by assembly of pillar[5]arenes mutifilms. *Anal. Chim. Acta* **2018**, *1036*, 49–57. [CrossRef] [PubMed]
24. Liu, Z.; Du, J.; Qiu, C.; Huang, L.; Ma, H.; Shen, D.; Ding, Y. Electrochemical sensor for detection of p-nitrophenol based on nanoporous gold. *Electrochem. Commun.* **2009**, *11*, 1365–1368. [CrossRef]
25. Madhu, R.; Karuppiah, C.; Chen, S.M.; Veerakumar, P.; Liu, S.B. Electrochemical detection of 4-nitrophenol based on biomass derived activated carbons. *Anal. Methods* **2014**, *6*, 5274–5280. [CrossRef]
26. Wang, H.B.; Li, Y.; Xu, M.T.; Dong, G.L.; Bai, H.Y. Porous Carbon Nanospheres for 4-aminophenol Detection based on Porous Carbon Nanospheres. *Xinyang Norm. Univ.* **2017**, *30*, 596–599.
27. Arvinte, A.; Mahosenaho, M.; Pinteala, M.; Sesay, A.; Virtanen, V. Electrochemical oxidation of p-nitrophenol using graphene-modified electrodes, and a comparison to the performance of MWNT -based electrodes. *Microchim Acta* **2011**, *174*, 337–343. [CrossRef]
28. Zhou, Y.Y.; Zhao, J.; Li, S.H.; Guo, M.J.; Fan, Z. Electrochemical Sensor for Detection of p-Nitrophenol Based on Cyclodextrin Decorated Gold Nanoparticles-Mesoporous Carbon Hybrid. *Analyst* **2019**, *144*, 4395–4399. [CrossRef]

29. Saadati, F.; Ghahramani, F.; Shayani-jam, H.; Piriet, F.; Yaftian, M.R. Synthesis and characterization of nanostructure molecularly imprinted polyaniline/graphene oxide composite as highly selective electrochemical sensor for detection of p -nitrophenol. *J. Taiwan Inst. Chem. Eng.* **2018**, *86*, 213–221. [CrossRef]
30. Li, C.; Wu, Z.; Yang, H.; Deng, L.; Chen, X. Reduced graphene oxide-cyclodextrin-chitosan electrochemical sensor: Effective and simultaneous determination of o- and p-nitrophenols. *Sens. Actuators* **2017**, *b251*, 446–454. [CrossRef]